

EPR SPECTROSCOPIC CHARACTERIZATION OF Cr^{V} - SACCHARIDE COMPLEXES

SIGNORELLA, S.*; GONZÁLEZ, J.C.; SALA, L.F.#

Departamento de Química, Facultad de Ciencias Bioquímicas y Farmacéuticas, UNR, Suipacha 531,
2000 Rosario, Argentina.

*signorel@infovia.com.ar; # inquirbir@satlink.com

Received: March 28, 2002. Accepted: April 23, 2002

CONTENTS

Abstract

1. Introduction
 2. Characterization of Cr^{V} bound to O-donors chelate ligands
 - 2.1 EPR spectroscopy of Cr^{V}
 - 2.2 Alditols
 - 2.3 Cyclic diols
 - 2.4 Methyl glycosides
 - 2.5 Hydroxy acids
 - 2.6 Aldohexoses
 - 2.7 Disaccharides
 - 2.8 Aldopentoses
 - 2.9 2-Deoxyaldoses
 - 2.10 Uronic acids
 3. Conclusions
- Acknowledgements
References

ABSTRACT

This review describes the characterization of Cr^{V} complexes formed with O-donor chelate ligands employing solution EPR spectroscopy. The discussion is particularly focused on Cr^{V} complexes formed with neutral and acid saccharides, although Cr^{V} complexes of 2-hydroxyacids and 1,2-diols are also described. The review emphasizes the pH dependence of the Cr^{V} speciation and the intramolecular competition of different functional groups and different orientations within the same functional group of saccharides for binding Cr^{V} .

INTRODUCTION

Cr^{VI} is a potential hazard both in a biological and an ecological context [1,2]. The observation of Cr^{V} intermediates in the selective oxidation of organic substrates by Cr^{VI} and their implication in the mechanism of Cr-induced cancers [3-5] has generated a considerable amount of interest in the chemistry and biochemistry of this Cr oxidation state [6-9]. The reduction of Cr^{VI} occurs with a wide variety of biological reductants [10-15]. The major coordination sites involved in Cr binding are hydroxo, alcoholato, carboxylato, and thiolato donors groups [2, 14]. Five-membered, O-donor, chelate ligands,

such as 1,2-diols and 2-hydroxy acids, are effective as non-enzymatic reductants and chelates for high Cr oxidation states [1,14,16]. The Cr^V speciation is pH dependent and the dependence of the formation of Cr^V complexes with different ligands types is likely to be important with respect to their biological activities. In particular, the knowledge of the Cr^V speciation at low pH values has relevance with respect to phagocytosis of insoluble chromates, where the pH of the vacuole becomes more acidic (pH = 4-5), and to the transport of Cr^V in soils [1-3]. The interaction with soil components facilitates the transport of chromium from chemical dumps to the environment through the formation of soluble and stable hypervalent chromium species contributing to the environmental pollution [3]. Carbohydrates constitute 5-20% (average 10%) of soil organic matter and they constitute more than 50% of dry matter in plants [17]. Because of their potential biological relevance, it is important to know the ability of saccharides to reduce or stabilize hypervalent Cr.

This review is centered mainly in the studies conducted in our research group and our results are discussed in the context of our own research and those of other laboratories. The review describes the Cr^V species formed by reaction of Cr^{VI} with diols, 2-hydroxyacids, alditols (ald-ol), aldoses (ald), deoxyaldoses (dald), glycosides (gly), disaccharides, aldonic (alda) and uronic acids, at room temperature, as well as Cr^V species generated (a) in the reaction of Cr^{VI} with cysteine (cys) or glutathione (GSH) stabilized by the presence of excess of saccharide, and (b) in the ligand-exchange reaction between the saccharide and [Cr^VO(ehba)₂].

2. CHARACTERIZATION OF CR^V BOUND TO O-DONORS CHELATE LIGANDS

2.1 EPR spectroscopy of Cr^V

The most common mean of characterizing Cr^V complexes in solution is EPR spectroscopy, where strong isotropic signals are observed at room temperature in X-band spectra. Typical Cr^V EPR spectra exhibit a single narrow signal (1-5 G) centered at $g_{iso} \sim 1.98$ with four weak ⁵³Cr (9.55% abundance, $I = 3/2$) hyperfine peaks. In the case of Cr^V-alcohol species, the central signal can be further split by superhyperfine (shf) coupling with the carbinolic hydrogen atoms (¹H $a_{iso} \sim 0.4 - 1.0 \times 10^{-4} \text{ cm}^{-1}$). An empirical relationship between the nature and number of donor groups and the EPR spectral parameters of Cr^V complexes has been established [18]. Five-co-ordinate Cr^V species show higher g_{iso} and lower ⁵³Cr A_{iso} values than the corresponding in six-co-ordinate species [18-20]. The assignment of the structures of new oxo-Cr^V species in solution can then be made according to the isotropic EPR parameters (g_{iso} and A_{iso} values) and the shf pattern of the signal [21-22]. The criteria for assigning the structures of the species described below rely on a number of independent observations. These include: a.- the [substrate] and [H⁺] dependences of the EPR signals resulting from the ligand-exchange reactions of Na[Cr^VO(ehba)₂] or from chelation of Cr^V generated in the reaction of Cr^{VI} with GSH or cys; b.- the [H⁺], [ligand] and [Cr^{VI}] dependences of the EPR signal intensities for the Cr^V complexes formed during the Cr^{VI} + substrate reaction and c.- empirical correlations between the known structure of Cr^V complexes and their EPR parameters. Together they provide evidence for the structure of the Cr^V complexes corresponding to the EPR signal.

2.2 Alditols

Polyols usually form weak complexes with metal cations. However, in order to compete with water molecules for the occupancy of the first co-ordination sphere of a metal cation, these acyclic ligands must possess some pre-organization and contain particular spatial arrangements of the ligating groups [23]. The *threo* arrangement of two vicinal hydroxy groups is particularly suitable for the complexation of hypervalent metal cations, which reinforces the CrO³⁺ preference to form five-membered Cr^V chelate

rings [24-26]. The redox and complexation chemistry of Cr^{VI}/alditol systems has been recently examined [27]. When an excess of alditol over Cr^{VI} is used, the secondary OH groups of the substrate are inert to oxidation and alditols are selectively oxidized by Cr^{VI} at the primary OH group to yield the aldonic acid as the only oxidation product. The reaction involves a Cr^{VI} → Cr^V → Cr^{III} reduction path and the relative rate of the Cr^{VI}/Cr^V and Cr^V/Cr^{III} steps depends of the [H⁺]. At [H⁺] > 0.1M the Cr^{VI}/Cr^V step is rate determining, while at pH > 1 the rate of the Cr^V/Cr^{III} reduction is the slow step.

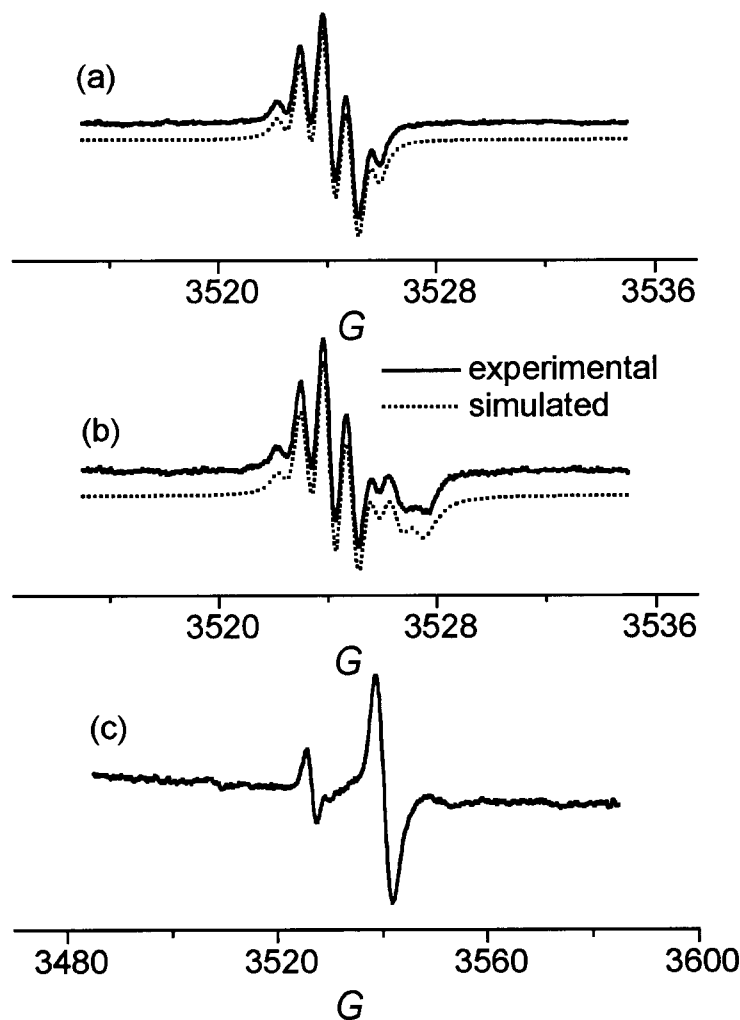


FIGURE 1. X-band EPR signal of solutions of glc-ol and Cr^{VI}. (a) glc-ol:Cr^{VI} = 10:1, pH = 5, mod. ampl. = 0.4 G; (b) glc-ol:Cr^{VI} = 20:1, pH = 2, mod. ampl. = 0.4 G; (c) glc-ol:Cr^{VI} = 10:1, [H⁺] = 0.1 M, mod. ampl. 1.01 G. *T* = 25°C, frequency = 9.7815 GHz. [Cr^{VI}] = 2.5 × 10⁻³ M.

Cr^V generated by redox reaction of Cr^{VI} with the alditol, is stabilized by the excess substrate or by the oxidation product (alda) and an estimation of the Cr^V species formed in the reaction can be made at different pH, [Cr^{VI}] and [ald-ol], according to the shf pattern and the isotropic EPR parameters [27]. The g_{iso} and A_{iso} values reveal that five- and six-co-ordinate oxo-Cr^V complexes are formed depending on the [H⁺]. At pH > 2, only five-co-ordinate Cr^V species form ($g_{iso} \approx 1.9799$, $A_{iso} \approx 16.5 \times 10^{-4} \text{ cm}^{-1}$),

intramolecular redox reactions are very slow and the Cr^{V} complexes remain in solution several days to weeks (Figure 1-a).

It is known that in Cr^{V} -diolato complexes formed with linear diols all the protons are equivalent in isotropic EPR spectra [28-29]. The shf structure of the EPR signal at g_{iso} 1.9799 (quintet) indicates that the five-coordinate oxo- Cr^{V} complexes formed with excess ald-ol involve metal binding to four secondary alcoholate donors, belonging to the *vic*-diolate donor sites of two bidentate ald-ol bound to Cr^{V} ($[\text{CrO}(\text{O},\text{O}\text{-ald-ol})_2]^-$, type A complex, Figure 2). It is interesting to note that the more stable oxo- Cr^{V} complexes do not involve Cr^{V} coordinated to the primary hydroxyl group. Besides $[\text{CrO}(\text{O},\text{O}\text{-ald-ol})_2]^-$, a second type of oxo- Cr^{V} bis-chelate (g_{iso} 1.9787) appears at pH 1–2 (Figure 1-b). The spectroscopic EPR parameters correspond to oxo- Cr^{V} species formed with the oxidation product (alda), with coordination occurring via the 1-carboxylate-2-hydroxy donor groups, $[\text{CrO}(\text{O}^-, \text{O}^2\text{-alda})_2]^-$ (type B complex, Fig. 2)). At $[\text{H}^+] \geq 0.1 \text{ M}$, positively charged six-co-ordinate Cr^{V} monochelates ($g_{\text{iso}} \approx 1.9719$, $A_{\text{iso}} \approx 20.0$, type C complex, Figure 2) form and are the dominant Cr^{V} species in solution (Figure 1-c).

2.3. Cyclic diols

The EPR studies of cyclic diol- Cr^{V} complexes reveal that the multiplicity of the EPR signal of Cr^{V} -diolate complexes is dependent upon whether the ligand is cyclically strained or not. The EPR shf pattern of Cr^{V} -cyclic diols systems was examined for the Cr^{V} -diolato₂ complexes formed by reduction

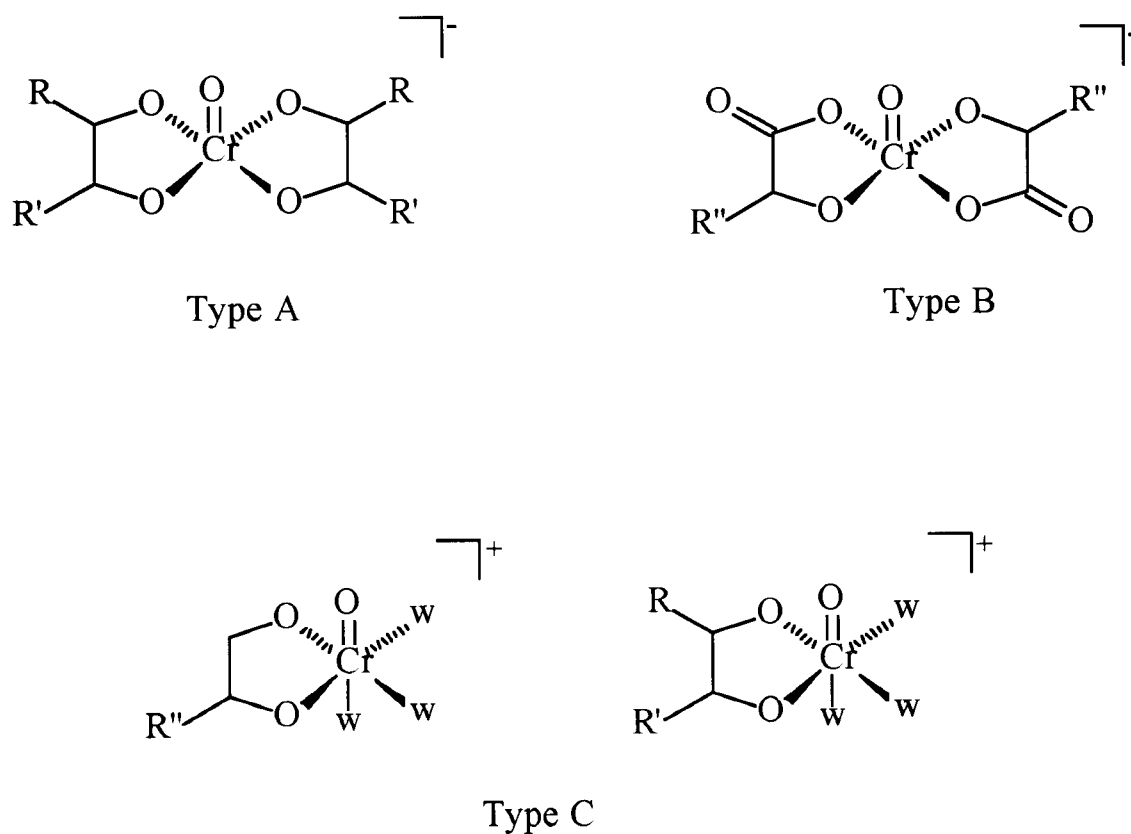


FIGURE 2. Cr^{V} species formed in the reaction between Cr^{VI} and alditols.

of Cr^{VI} by GSH in the presence of *cis*- or *trans*-1,2-cyclohexanediol [2,30]. It was observed that the strain of the six-member ring imparts inequality to the magnetic environment of the protons in the second co-ordination sphere. *Trans*-1,2-cyclohexanediol affords a singlet corresponding to [CrO(*trans*-1,2-cyclohexanediolato)₂]⁻ (g_{iso} 1.9800), while the *cis* isomer affords two triplets corresponding to the two geometric isomers of [Cr^V(O)(*cis*-1,2-cyclohexanediolato)₂]⁻, each with two equivalent ¹H_{eq} coupled to the Cr^V electronic spin (g_{iso} 1.9799, ¹H a_{iso} 0.97×10^{-4} cm⁻¹; g_{iso} 1.9796, ¹H a_{iso} 0.89×10^{-4} cm⁻¹) (Figure 3) [30]. The different EPR shf pattern is explained considering that when protons lay in the Cr^V-ligand plane there is a maximal overlap between the proton orbital and the Cr^V orbital containing the unpaired electron density [21]. In the EPR spectral simulations, values for ¹H a_{iso} are included only where the ¹H a_{iso} value is greater than the LW (line width) of the Cr^V species, since the signal is not significantly affected where the ¹H a_{iso} value is \leq LW. Consequently, the singlet observed for the *trans*-isomer means that the two carbinolic protons are very weakly coupled to the Cr^V electronic spin resulting in a ¹H $a_{\text{iso}} < \text{LW}$.

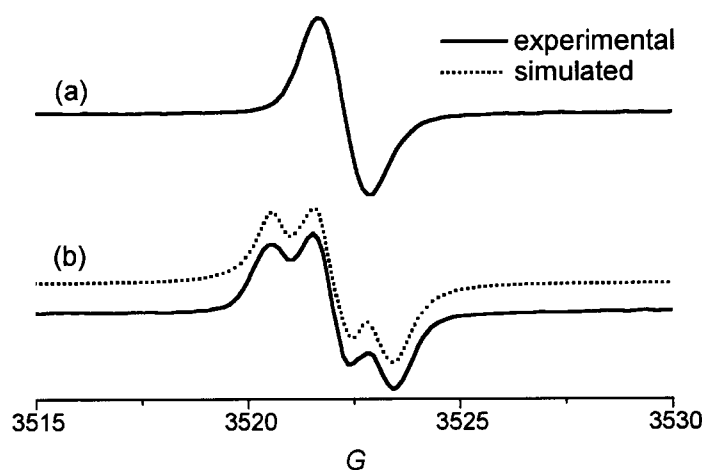


FIGURE 3. X-band EPR spectra of mixtures of (a) GSH:Cr^{VI}:*trans*-1,2-cyclohexanediol = 1:1:10000, frequency = 9.7743 GHz., mod. ampl. = 0.4 G; (b) GSH:Cr^{VI}:*cis*-1,2-cyclohexanediol = 1:1:10000, frequency = 9.7739 GHz., mod. ampl. = 0.2 G. [Cr^{VI}] = 0.25 mM, pH 7.5.

The study of Cr^V-diolate complexes formed by reduction of Cr^{VI} by GSH in the presence of *cis*- or *trans*-1,2-cyclopentenediol extends the analysis of the EPR shf pattern to Cr^V-diolate species formed between Cr^V and five-membered ring 1,2-diols [22]. Unlike Cr^V complexes formed with *cis*- and *trans*-1,2-cyclohexanediol, 1,2-cyclopentenediols afford [CrO(*cis*-1,2-cyclopentenediolate)₂]⁻ and [CrO(*trans*-1,2-cyclopentenediolate)₂]⁻ with indistinguishable EPR spectral patterns (Figure 4) corresponding to two Cr^V components split by non equivalent carbinolic protons coupled to the Cr^V electronic spin: one Cr^V component (g_{iso} 1.9803/4, A_{iso} 15.9×10^{-4} cm⁻¹) with two "pseudo-equatorial" protons (¹H a_{iso} 0.84, 0.81×10^{-4} cm⁻¹ (*cis*-diolate) and 0.84, 0.76×10^{-4} cm⁻¹ (*trans*-diolate)) and two protons disposed at angles in between the "pseudo-axial/equatorial" orientations, and a second Cr^V species (g_{iso} 1.9798/99, A_{iso} 15.9×10^{-4} cm⁻¹) with two "pseudo-axial" protons (¹H a_{iso} 0.41, $< \text{LW}$ (*cis*-diolate) and 0.47, $< \text{LW}$ (*trans*-diolate)), and two protons protruding at intermediate angles. Low modulation amplitude and very large (5000 times) excess of diol over Cr^V are required for the shf pattern of the EPR signal of the Cr^V-1,2-pentenediol species resolves [22].

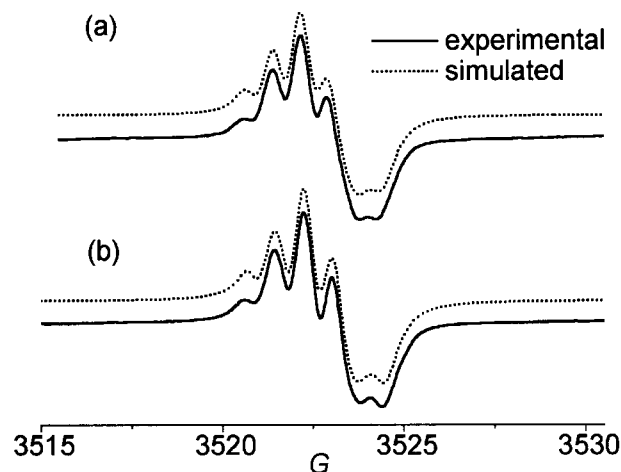


FIGURE 4. X-band EPR spectra of mixtures of (a) GSH:Cr^{VI}:*trans*-1,2-cyclopentanediol = 1:1:5000, [Cr^{VI}] = 1.0 mM, frequency = 9.7620 GHz., mod. ampl. = 0.4 G; (b) GSH:Cr^{VI}:*cis*-1,2-cyclopentanediol = 1:1:5000, [Cr^{VI}] = 0.5 mM, frequency = 9.7634 GHz., mod. ampl. = 0.4 G.

It results evident that the $[\text{Cr}^{\text{V}}(\text{O})(1,2\text{-cyclohexanediolate})_2]^-$ system differentiates the axially and equatorially disposed carbinolic protons, and consequently, the resulting shf coupling corresponds to the maximal and minimal values expected for the ^1H coupled to the Cr^{V} electronic spin; while the strained bi-cycle arising from the two fused five-membered rings in $[\text{Cr}^{\text{V}}(\text{O})(1,2\text{-cyclopentanediolato})_2]^-$ yields isotropic EPR spectra corresponding to the average conformations of two geometric isomers in which all the carbinolic protons are non equivalent.

For either the 1,2-cyclopentanediol/ Cr^{V} or 1,2-cyclohexanediol/ Cr^{V} systems, it was found that CrO^{3+} shows a marked preference for binding to the *cis*- rather than the *trans*-diol groups of the cyclic diol [22,30].

2.4. Methyl glycosides

The preference of CrO^{3+} for binding *cis*- rather than *trans*-diol groups was confirmed by experiments where Cr^{V} was generated by reaction of Cr^{VI} with *cys* in the presence of excess of methyl glycoside and in the ligand-exchange reaction of the glycosides with $[\text{Cr}^{\text{V}}\text{O}(\text{ehba})_2]^-$ [31-32]. It was observed that at pH 5.5 and 7.5 an EPR signal appears when excess methyl D-galactopyranoside (gal1Me) or methyl D-mannopyranoside (man1Me) is added to a *cys*: Cr^{VI} equimolar mixture but not upon addition of excess methyl D-glucopyranoside (glc1Me) or methyl D-xilopyranoside (xil1Me). The potential binding modes in these cyclic glycosides to afford five-membered Cr^{V} species are the 2,3-*cis*- and 3,4-*trans*-diolato moieties in man1Me, the 2,3-*trans* and 3,4-*cis*-diolate moieties in gal1Me, the 2,3-*trans* and 3,4-*trans*-diolato moieties in glc1Me and the 2,3-*trans*-diolate moieties in xil1Me. The observation of the EPR signal only for man1Me and gal1Me evidences the higher ability of the *cis* vs the *trans*-diolate for binding Cr^{V} . This result was taken as the base for the interpretation of the EPR spectral features of man1Me and gal1Me/ Cr^{V} mixtures in terms of Cr^{V} -diolate species involving mainly binding through O^2, O^3 -man1Me and O^3, O^4 -gal1Me. The contribution to the EPR signals from other species, involving O^3, O^4 -man1Me and O^2, O^3 -gal1Me, was considered to be small or negligible.

A low intensity EPR singlet at $g_{\text{iso}} 1.9792$ is observed at the early stages of the ligand-exchange reactions of $[\text{Cr}^{\text{V}}\text{O}(\text{ehba})_2]^-$ with xil1Me and glc1Me in HEPES buffer (pH 7.5) with the g_{iso} value and

multiplicity expected for $[\text{Cr}^{\text{V}}\text{O}(\text{ehba})(\text{trans-O,O-sugar})]^-$ ($g_{\text{calc}} 1.9791$) [32]. With time, this singlet is replaced by another weak singlet at $g_{\text{iso}} 1.9799$ due to $[\text{Cr}^{\text{V}}\text{O}(\text{trans-O,O-gly1Me})_2]^-$ ($g_{\text{calc}} 1.9800$). The relatively poor ability of the *trans*-diolato groups to bind Cr^V means the disproportionation of $[\text{Cr}^{\text{V}}\text{O}(\text{ehba})_2]^-$ (which is fast at pH 7.5) [9] occurs much faster than the ligand-exchange reaction with the result that the $[\text{Cr}^{\text{V}}\text{O}(\text{ehba})_2]^-$ EPR signal quickly disappears and only a very weak $[\text{Cr}^{\text{V}}\text{O}(\text{O,O-gly1Me})_2]^-$ signal is observed in the final spectrum. Similarly, the $[\text{Cr}^{\text{V}}\text{O}(\text{O,O-gly1Me})_2]^-$ EPR signal is not observed for the Cr^{VI}/cys reaction in the presence of excess xil1Me or glc1Me because the cys/Cr^V redox reaction [33] is much faster than the Cr^V-cys ligand-exchange reactions with these glycosides. From these results it was concluded that kinetic control favors the formation of Cr^V-diolato species of *cis*- over *trans*-diolato moieties of six-membered sugar rings [32].

The Cr^{VI}/cys reaction in the presence of excess α -man1Me or $\alpha(\beta)$ -gal1Me, at pH 5.5 or 7.5, affords two EPR triplets (shown in Figure 5-a) at $g_{\text{iso1}} 1.9802$ and $g_{\text{iso2}} 1.9800/1$ ($A_{\text{iso}} 16.5(3) \times 10^{-4} \text{ cm}^{-1}$, $\sim 50:50 g_{\text{iso1}}/g_{\text{iso2}}$ ratio). The g_{iso} and A_{iso} values and the shf splitting –the triplet means that two (one from each chelate ring) carbinolic protons are coupled to the Cr^V electronic spin- are consistent with the presence of the two geometrical isomers of $[\text{Cr}(\text{O})(\text{cis-O,O-gly1Me})_2]^-$ (I-II with man1Me and III-IV with gal1Me, Figure 6).³² The formation of $[\text{Cr}(\text{O})(\text{cis-O,O-gly1Me})_2]^-$ was found to be faster at pH 5.5 than at pH 7.5, and it was interpreted as the consequence of the faster generation of Cr^V from the redox reaction between cys and Cr^{VI} at the lower pH value [33].

Figure 5-b,c show the EPR spectra taken at the beginning of the ligand-exchange reaction of the methyl glycoside. At pH 7.5, the rapid ligand-exchange reaction of $[\text{CrO}(\text{ehba})_2]^-$ with excess α -man1Me or $\alpha(\beta)$ -gal1Me affords the two geometric isomers of $[\text{Cr}^{\text{V}}\text{O}(\text{cis-O,O-gly1Me})_2]^-$ as the final Cr^V species observed in the EPR spectra in a $\sim 50:50 g_{\text{iso1}}/g_{\text{iso2}}$ ratio. At pH 5.5, ligand-exchange reactions of $[\text{CrO}(\text{ehba})_2]^-$ with excess α -man1Me or $\alpha(\beta)$ -gal1Me are not complete and after 2 h >50% of the total Cr^V is $[\text{CrO}(\text{ehba})_2]^-$, while oxo-Cr^V-diolato₂ species represent $\sim 5\%$ of total Cr^V. A fact attributed, in part, to the lower reactivity of $[\text{CrO}(\text{ehba})_2]^-$ toward disproportionation and ligand exchange at the lower pH values.

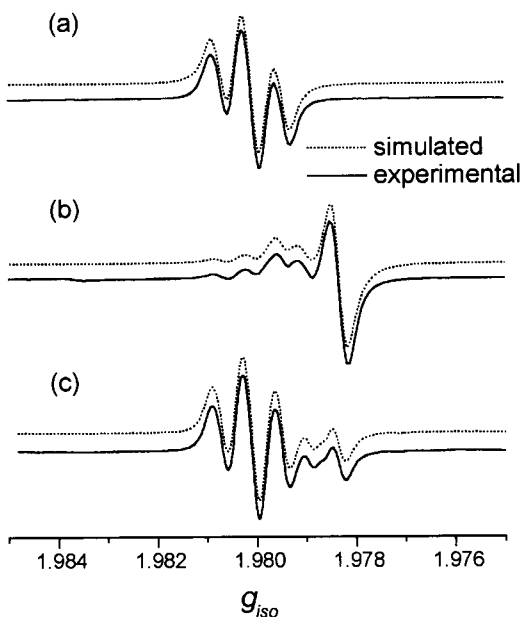


FIGURE 5. X-band EPR spectra of mixtures of (a) cys:Cr^{VI}: α man1Me = 1:1:100, pH 5.5; $t = 120$ min; (b) $[\text{Cr}^{\text{V}}\text{O}(\text{ehba})_2]^-$: α man1Me = 1:100, pH 5.5, $t = 3$ min; (c) $[\text{Cr}^{\text{V}}\text{O}(\text{ehba})_2]^-$: α man1Me = 1:100, pH 7.5, $t = 3$ min. $T = 25^\circ\text{C}$, frequency ≈ 9.67 GHz, mod. ampl. = 0.2 G.

Under more acidic conditions ($\text{pH} < 1$), gly1Me reduces both Cr^{VI} and Cr^{V} . Complexation of Cr^{V} takes place prior to the redox paths, but the distribution of Cr^{V} species is rather different than at $\text{pH} \geq 5.5$. In the reaction of α -man1Me with Cr^{VI} , at $\text{pH} \leq 1$ and a 10:1 α -man1Me: Cr^{VI} ratio, the EPR spectrum is composed of a triplet at $g_{\text{iso}1}$ 1.9800, a doublet at $g_{\text{iso}2}$ 1.9798, and three signals with no shf structure at $g_{\text{iso}3}$ 1.9788, $g_{\text{iso}4}$ 1.9746 and $g_{\text{iso}5}$ 1.9716 [31]. The intensity of signals at $g_{\text{iso}4}$ and $g_{\text{iso}5}$, relative to those of the $g_{\text{iso}1}$, $g_{\text{iso}2}$ and $g_{\text{iso}3}$ signals, increases with higher $[\text{H}^+]$ and at $[\text{H}^+] > 0.3 \text{ M}$ the signal at $g_{\text{iso}5}$ is the dominant one and is attributed to six-coordinate $[\text{CrO}(\text{O}^4, \text{O}^6\text{-man1Me})(\text{OH}_2)_3]^+$ monochelates ($g_{\text{calc}} = 1.9724$). Among the six-co-ordinate complexes, **V** (Figure 6) is proposed to be the precursor of the redox steps. The results show that the formation of positively charged Cr^{V} -monochelates are favored in acid medium and low glycoside: Cr^{VI} ratios, while the formation of anionic Cr^{V} -bis-chelates are favored at the higher pH and larger glycoside: Cr^{VI} ratios.

2.5. Hydroxy acids

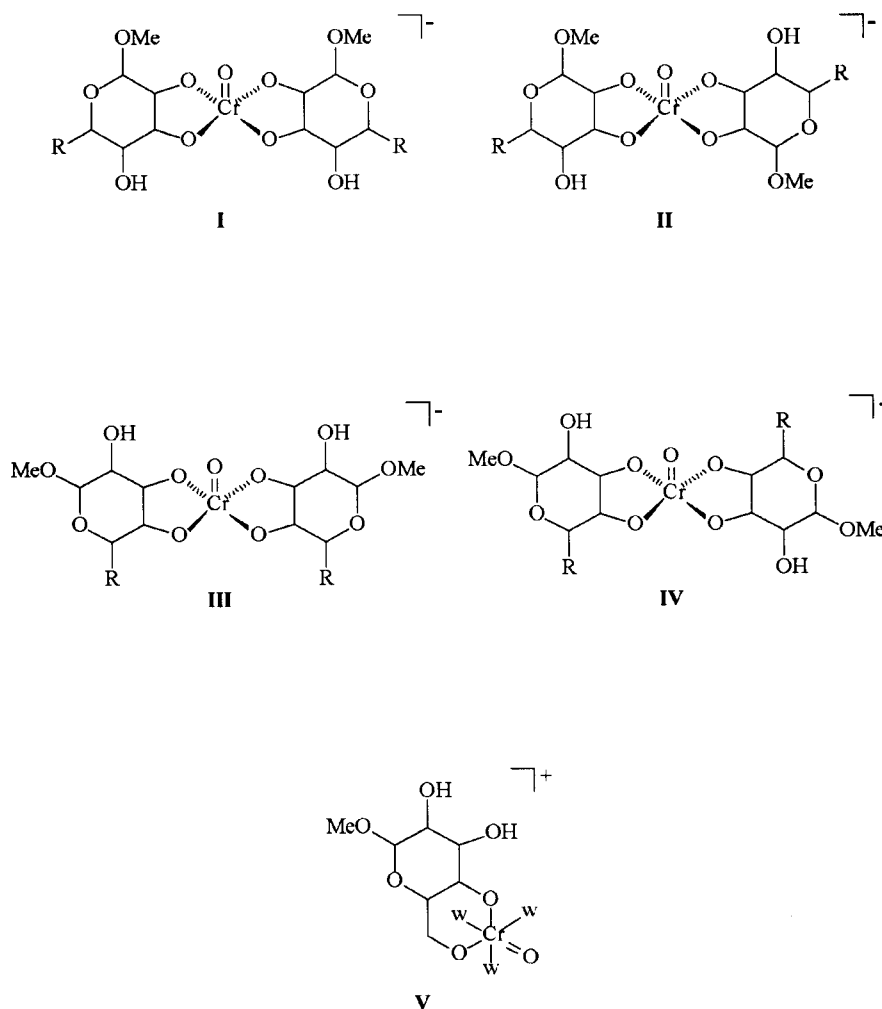
The relatively stable Cr^{V} -2-hydroxycarboxylato complexes $(\text{Na}[\text{Cr}^{\text{V}}\text{O}(\text{ehba})_2])$ ($\text{ehba} = 2\text{-ethyl-2-hydroxybutanoate}(2\text{-})$) and $(\text{K}[\text{Cr}^{\text{V}}\text{O}(\text{hmba})_2])$ ($\text{hmba} = 2\text{-hydroxy-2-methylbutanoate}(2\text{-})$) were the first studied as model compounds of Cr^{V} biological activity [34-35]. $(\text{K}[\text{CrO}(\text{hmba})_2])$ and $(\text{Na}[\text{CrO}(\text{ehba})_2])$ have been isolated and their structure determined by X-ray diffraction [36-38]. These complexes have distorted trigonal bipyramidal coordination geometry, with carboxylate and alcoholate donors occupying the axial and equatorial sites, and the remaining equatorial site occupied by an oxo ligand. The stability of these complexes in aqueous solution ranges from minutes to days depending of the pH but they are very stable in aprotic solvents. EPR and ^1H ENDOR studies revealed the presence of more than one geometrical isomer of these complexes in solution ($([\text{CrO}(\text{O}^1, \text{O}^2\text{-hmba})_2])^-$: g_{iso} 1.9785, A_{iso} $17.4 \times 10^{-4} \text{ cm}^{-1}$; g_{iso} 1.9785, A_{iso} $16.3 \times 10^{-4} \text{ cm}^{-1}$. $([\text{CrO}(\text{O}^1, \text{O}^2\text{-ehba})_2])^-$: g_{iso} 1.9784, A_{iso} $17.2 \times 10^{-4} \text{ cm}^{-1}$; g_{iso} 1.9784, A_{iso} $16.1 \times 10^{-4} \text{ cm}^{-1}$).^{19,39} Cr^{V} -hmba₂ intermediate complexes are also formed in the $\text{Cr}^{\text{VI}} + \text{hmba}$ reaction in 0.25 – 1.0 M acid solutions, where they rapidly decay to the redox products [40].

$(\text{K}[\text{CrO}(\text{qa})_2] \cdot \text{H}_2\text{O})$ ($\text{qa} = 1\text{R}, 3\text{R}, 4\text{R}, 5\text{R}-1, 3, 4, 5\text{-tetrahydroxycyclohexane carboxylic acid}$) has been isolated and the analysis of the XAFS data shows a coordination geometry analogous to that of $(\text{K}[\text{CrO}(\text{hmba})_2])$ and $(\text{Na}[\text{CrO}(\text{ehba})_2])$ [41]. In aqueous solutions of $\text{pH} < 4.0$, $(\text{K}[\text{CrO}(\text{qa})_2] \cdot \text{H}_2\text{O})$ gives two EPR signals (g_{iso} 1.9787, A_{iso} $17.2 \times 10^{-4} \text{ cm}^{-1}$; g_{iso} 1.9791, A_{iso} $16.4 \times 10^{-4} \text{ cm}^{-1}$) which are consistent with those found for $(\text{K}[\text{CrO}(\text{hmba})_2])$ and $(\text{Na}[\text{CrO}(\text{ehba})_2])$ and are assigned to the two geometrical isomers of the $([\text{CrO}(\text{O}^1, \text{O}^7\text{-qa})_2])^-$ linkage isomer [21]. At $\text{pH} 5.0\text{-}7.5$, solution EPR spectroscopic studies show that quinic acid is able to coordinate Cr^{V} by either the 2-hydroxyacid and/or the diolate moieties. In this pH range, three additional signals appear (g_{iso} 1.9791, 1.9794 and 1.9799) which have EPR spectral data consistent with the presence of $([\text{CrO}(\text{O}^1, \text{O}^7\text{-qa})(\text{O}^3, \text{O}^4\text{-qa})])^-$ and $([\text{CrO}(\text{O}^1, \text{O}^7\text{-qa})(\text{O}^4, \text{O}^5\text{-qa})])^-$, with $([\text{CrO}(\text{O}^1, \text{O}^7\text{-qa})(\text{O}^3, \text{O}^4\text{-qa})])^-$ being the major species in solution in this pH range. At pH values > 7.5 , the Cr^{V} -qa EPR spectra show two triplets (g_{iso} 1.9800 and g_{iso} 1.9802) which are ascribed to the geometric isomers of the bis-diol Cr^{V} -qa complex, $([\text{CrO}(\text{O}^3, \text{O}^4\text{-qa})_2])^-$. This assignment was supported by the similarity of the EPR spectral data with those formed in the reduction of Cr^{VI} by GSH in the presence of shikimic acid (sa , 3R,4R,5R-3,4,5-trihydroxycyclohexenecarboxylic acid) which does not possess a 2-hydroxyacid moiety.²¹ At $\text{pH} > 5.5$, the EPR spectra reveal that two Cr^{V} -sa species forms with g_{iso} 1.9800 and 1.9801, ascribed to the two geometric isomers of $([\text{CrO}(\text{O}^3, \text{O}^4\text{-sa})_2])^-$, with no alternative linkage isomers present in significant concentrations.

The redox reaction of lactic acid (la) with Cr^{VI} involves Cr^{V} as a redox intermediate [42]. At $\text{pH} 4.5$, the EPR spectra (Figure 7) show two triplets (g_{iso} 1.9787, $^1\text{H } a_{\text{iso}}$ $0.52 \times 10^{-4} \text{ cm}^{-1}$; g_{iso} 1.9783, $^1\text{H } a_{\text{iso}}$ $0.60 \times 10^{-4} \text{ cm}^{-1}$) with spectral parameters consistent with those expected for the two geometrical isomers of $([\text{CrO}(\text{O}^1, \text{O}^2\text{-la})_2])^-$ [43].

Naturally occurring acid saccharides are relevant ligands well suited for stabilization of Cr^{V} since

they possess the possibility of 2-hydroxycarboxylato and vic-diolato potential chelate sites for Cr^V. It was found that five coordinated oxo-Cr^V complexes are formed in the oxidation of galactonic acid (gala) by Cr^{VI} [44]. The redox reaction occurs through Cr^{VI} → Cr^{III} and Cr^{VI} → Cr^V → Cr^{III} paths. The rate of reduction of both Cr^{VI} and Cr^V is first order on [gala] and is catalyzed by protons. Cr^V is formed in a rapid step by reaction of Cr^{VI} with the CO₂^{•-} radical generated in the reaction. The EPR spectra show that several intermediate [Cr(O)(gala)₂]⁻ linkage isomers are formed in rapid pre-equilibria before the redox steps. In the 2-6 pH range, the EPR signals are composed of one triplet (*g*_{iso} 1.9781) and one double triplet (*g*_{iso} 1.9788), which have EPR spectral data consistent with the presence of [Cr(O)(O¹,O²-gala)₂]⁻ (**VI**, Figure 8) and [Cr(O)(O²⁽⁴⁾,O³⁽⁵⁾-gala)(O¹,O²-gala)]⁻ (**VII**). The relative proportion of the signals depends on the pH, but is independent of the reaction time. At pH 6-8, [Cr(O)(O²⁽⁴⁾,O³⁽⁵⁾-gala)(O¹,O²-gala)]⁻ is still present, but the major species corresponds to [Cr(O)(O²⁽⁴⁾,O³⁽⁵⁾-gala)₂]⁻ (**VIII**, *g*_{iso} 1.9795, quintet). At pH 7.4, the last complex represents the 92% of the total Cr^V in the reaction mixture. These results show that at the higher pH, the Cr^V-diolate binding mode is preferred over the Cr^V-2-hydroxyacid coordination mode, such as observed for the Cr^V/qa system.



R = CH₂OH, w = water

FIGURE 6. Oxo-Cr^V chelates formed with gly1Me.

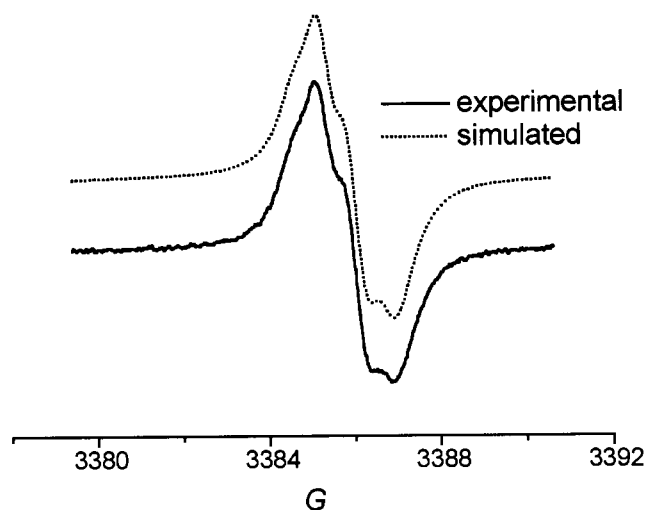


FIGURE 7. X-band EPR spectra of a mixture of la and Cr^{VI} . $T = 25^\circ\text{C}$, $\text{pH} = 4.5$, mod. ampl. = 0.4 G, frequency = 9.3759 GHz. $[\text{Cr}^{\text{VI}}] = 4.8 \times 10^{-4}$ M. la: $\text{Cr}^{\text{VI}} = 7000:1$.

Cr^{V} was observed in the reaction between gluconic acid (glca) and Cr^{VI} [44,45]. In aqueous solutions of $\text{pH} 2 - 6$, the Cr^{VI} oxidation of glca affords only one Cr^{V} species with EPR spectral parameters attributable to $[\text{Cr}(\text{O})(\text{O}^{2(3)}, \text{O}^{3(4)}\text{-glca})(\text{O}^1, \text{O}^2\text{-glca})]^-$ [44].

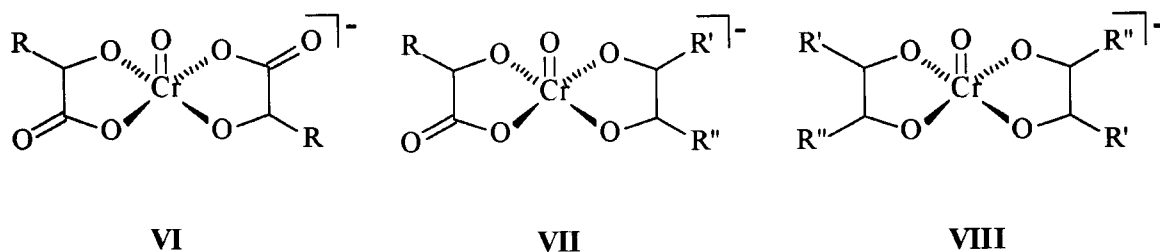


FIGURE 8. Five-coordinated oxo- Cr^{V} bis-chelates formed in the reaction between Cr^{VI} and gala. $\text{R} = \text{C}_4\text{H}_9\text{O}_4$, $\text{R}' = \text{CO}_2$, $\text{R}'' = \text{C}_3\text{H}_7\text{O}_3$ or $\text{R}' = \text{C}_3\text{O}_4\text{H}_4$, $\text{R}'' = \text{CH}_2\text{OH}$, for the $\text{Cr}^{\text{V}}\text{-O}^2, \text{O}^3\text{-gala}$ and $\text{Cr}^{\text{V}}\text{-O}^4, \text{O}^5\text{-gala}$ coordination modes.

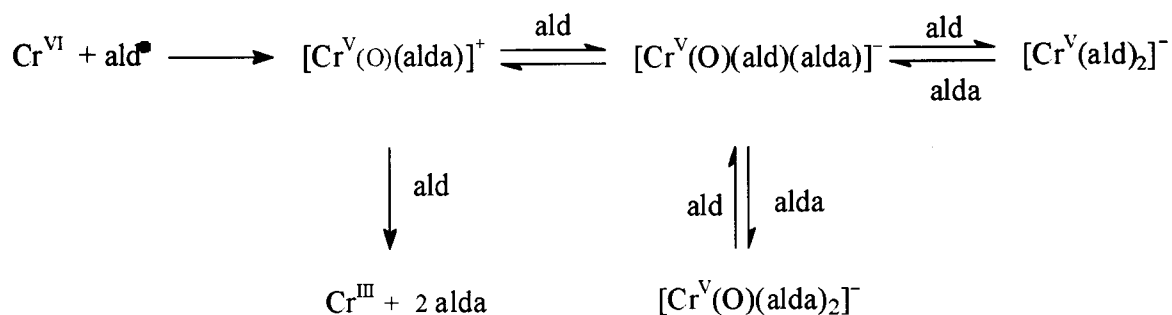
EPR spectroscopy was used to monitor the oxidation of D-ribonic acid (riba) by Cr^{VI} at $[\text{H}^+] > 0.1\text{M}$.⁴⁶ The EPR spectra consist of a single detectable sharp signal at $g_{\text{iso}} 1.978$, attributable to $[\text{Cr}^{\text{V}}(\text{O})(\text{O}^1, \text{O}^2\text{-riba})_2]$. At this $[\text{H}^+]$, the Cr^{V} signal grows and decays rapidly with time to yield the broad Cr^{III} signal ($g_{\text{iso}} 1.981$) as the ultimate fate of chromium in this reaction.

In the reaction of 4-hydroxybutyric acid with Cr^{VI} , Cr^{V} is not observed [47], a result which reinforces the fact that the 2-hydroxy-1-carboxylato moiety is the best suited to stabilize Cr^{V} by forming five-membered chelates.

2.6. Aldohexoses

In acid medium, aldohexoses are selectively oxidized by Cr^{VI} at the C1-OH hemiacetalic function yielding the aldonic acid (and/or the aldolactone) and Cr³⁺ as final products when an excess of sugar over Cr^{VI} is used [48-52]. The redox reaction occurs through Cr^{VI} → Cr^V → Cr^{III} and Cr^{VI} → Cr^V → Cr^{III} paths [49-51]. In 0.75 M [H⁺], D-glucose (glc), D-allose (allo), D-mannose (man) and D-galactose (gal) are oxidized at comparable rate by Cr^{VI} and Cr^V, specially at high [ald] [49]. The observed rate constants for the reduction of Cr^{VI} and Cr^V by the aldoses (k_6 and k_5) depend on [H⁺]. When the excess of sugar over Cr^{VI} is large, $k_6 < k_5$ at high [H⁺], but the relative values of the kinetic parameters reverse ($k_5 < k_6$) at high pH. At pH > 2, the Cr^V reduction rate becomes extremely slow and Cr^V species generated in the Cr^{VI} + ald reaction remain in solution for long time [18, 49, 52]. The EPR spectra show that a mixture of five-co-ordinate oxo-Cr^V bis-chelates ($g_{iso} \approx 1.979$, $A_{iso} 16.4(3) \times 10^{-4} \text{ cm}^{-1}$) are formed, and the relative proportion of each species in the reaction mixture depends on the reaction extent for each particular sugar [49]. For the glc + Cr^{VI} reaction, the EPR spectra show one triplet at g_{iso} 1.9789 and one quartet at g_{iso} 1.9793, with spectral parameters consistent with those expected for [CrO(O¹, O²-glc)(cis-O¹, O²-glc)]⁻ and [CrO(cis-O¹, O²-glc)(O²⁽³⁾, O³⁽⁴⁾-glc)]⁻. The man + Cr^{VI} reaction affords one triplet at g_{iso} 1.9791 and one quartet at g_{iso} 1.9795, which can be assigned to [CrO(cis-O¹⁽²⁾, O²⁽³⁾-man)(O¹, O²-mana)]⁻ and [CrO(cis-O¹⁽²⁾, O²⁽³⁾-man)(O³, O⁴-mana)]⁻ (mana = D-mannonic acid). Allo yields two triplets at 1.9794 ([CrO(cis-O^{1(2,3)}, O^{2(3,4)}-allo)₂]⁻) and 1.9785 ([CrO(O¹, O²-allo)₂]⁻); alloa = D-allonic acid). In the gal + Cr^{VI} system, the two main species present in solution are [CrO(cis-O³, O⁴-gal)(O²⁽⁴⁾, O³⁽⁵⁾-gala)]⁻ (quartet at g_{iso} 1.9789) and [CrO(O²⁽⁴⁾, O³⁽⁵⁾-gala)₂]⁻ (quintet at g_{iso} 1.9796). The observation of mixed Cr^V-ald-alda and/or Cr^V-alda₂ species with the open-chain alda bound to Cr^V via the vic-diolate for glc, gal and man, but not for allo (the only observed binding mode for alloa is via the 2-hydroxy-1-carboxylato moiety- was taken as a point of evidence for the preferential Cr^V chelation of *threo*- vs *erythro*-diolate moiety.

At [H⁺] ≥ 0.1 M, the reaction of Cr^{VI} with excess aldose affords two or three new EPR signals (g_{iso} 1.974, 1.971 and 1.966) besides the signal at g 1.979 [49,51]. The g_{iso} values of the new species are consistent with those expected for six-coordinated oxo-Cr^V complexes. The relative intensity of the Cr^V EPR signals depends on the [H⁺], but is independent of the ald:Cr^{VI} ratio employed, and, at [H⁺] > 0.75 M, the six-coordinated species are the major ones. The six- and five-coordinated oxo-Cr^V species decay at essentially the same rate, which means that these complexes are in rapid equilibrium and react at the same rate to yield the redox reactions. Scheme 1 summarizes the observed Cr^V-sugar redox and complexation chemistry. The proposed first step in the scheme is the formation of a six-coordinated oxo-Cr^V which can yield either the redox products or the Cr^V bis-chelates depending of the [H⁺]. When the [H⁺] is high, the redox reaction –which is acid catalyzed- is faster than complexation by a second molecule of the aldose; but as the [H⁺] decreases, complexation competes favorably with the redox reaction and five-coordinated Cr^V bis-chelates form and stabilize.



Scheme 1. Redox and complexation chemistry of Cr^V in the Cr^{VI}/aldose reaction

Five- and six-coordinated oxo-Cr^V species are also formed in 50 – 100 % acetic acid solutions of L-rhamnose and Cr^{VI} (10:1 ratio), with g_{iso} 1.978 and 1.973, respectively [53]. In aqueous solutions, the five-coordinated oxo-Cr^V species are observed at $g_{\text{iso}} \approx 1.977$ ($A_{\text{iso}} 16.4 \times 10^{-4} \text{ cm}^{-1}$) and prevail at pH 3-7 [51]. The six-coordinated oxo-Cr^V species have $g_{\text{iso}} \approx 1.970$ and dominate the EPR spectra at pH < 1.

The reduction of Cr^{VI} by α -D-glucose and β -D-glucose was studied in dimethylsulfoxide in the presence of pyridinium p-toluensulphonate, a medium where mutarotation is slower than the redox reaction [48]. The two anomers reduce Cr^{VI} and Cr^V by formation of an intermediate Cr^{VI} (and Cr^V) ester precursor of the slow redox step. The equilibrium constant for the formation of the intermediate chromic ester and the rate of the redox steps are different for each anomer. α -D-glucose forms the Cr^{VI}-glc ester with a higher equilibrium constant than β -D-glucose, but the electron-transfer within this complex is slower than for the β -anomer. The difference is attributed to the better chelating ability of the 1,2-cis-diolate moiety of the α -anomer. The EPR spectra show that the α -anomer forms several five-co-ordinate Cr^V bis-chelates with g_{iso} 1.9820 ($A_{\text{iso}} 15.9 \times 10^{-4} \text{ cm}^{-1}$), 1.9785 and 1.9756, while β -D-glucose affords a mixture of six-co-ordinate Cr^V monochelate (g_{iso} 1.9700) and five-coordinated Cr^V bis-chelates (g_{iso} 1.9820, $A_{\text{iso}} 15.8 \times 10^{-4} \text{ cm}^{-1}$, 1.9789 and 1.9767). The fact that the six-coordinated oxo-Cr^V monochelates are observed only when the β -anomer is used was interpreted as evidence for the binding of the *trans*-1,2-diolate moiety of the β -anomer vs the *cis*-1,2-diolate moiety of the α -anomer. The last affords a bis-chelate easier than the former because of the enhanced ability of the *cis*-1,2-diolate to bind Cr^V.

Complex EPR signals have been obtained from the ligand-exchange reaction between [CrO(ehba)₂] and glc [18]. The resulting Cr^V-glc solutions have been analyzed by using Q-, X- and S-band EPR spectroscopies and partially or fully deuterated glc. The Q-band EPR spectra of Cr^V/H₅-glc-C solutions were shown to contain at least six Cr^V species [54].

2.7. Disaccharides

The observation of long lived lactose/Cr^V species generated by direct reaction of Cr^{VI} with lactose in milk contaminated with chromates pointed out the capability of these compounds to stabilize Cr^V [55]. Further work revealed that disaccharides form stable hypervalent chromium chelates at pH > 2, while at higher [H⁺] their oxidation by Cr^{VI}/Cr^V is favoured [56]. When excess disaccharide over Cr^{VI} is used, the oxidation occurs selectively at the hemiacetalyc C¹OH group, with first-order kinetics on both [Cr^{VI}] and [disaccharide] [56]. The redox and complexation chemistry observed for the disaccharide-Cr^{VI} systems parallels that of aldoses. However, the glycoside moiety can retard the redox rate of the aglycone when additional binding to Cr^{VI} by the glycoside moiety is possible. In the case of maltose (mal), this effect reduce the observed rate constant to one half of the value obtained for glc [56]. The relative ability of four disaccharides to reduce Cr^{VI}, melibiose (mel) > lactose (lac) > cellobiose (cel) > mal, was attributed to the increasing stability of the intermediate disaccharide-Cr^{VI} chelates formed with mel through mal. EPR spectroscopy was used to determine the Cr^V species formed in the reaction of Cr^{VI} with mel, lac, cel and mal or in the reaction of Cr^{VI} with GSH in the presence of excess disaccharide, in the 5-7 pH range [56]. The EPR spectral features of disaccharide/Cr^V mixtures were interpreted in terms of Cr^V-diolato species involving mainly Cr^V binding through the *cis*-O¹,O²-diolato of mal and cel and the *cis*-O¹,O²-diolato and *cis*-O³,O⁴-diolato of lac and mel.

In 0.2 M HClO₄ the EPR spectra of the reaction between lac and Cr^{VI} show three signals at g_{iso} 1.9797, 1.9743 and 1.9715 (Figure 9-a). The signal at g_{iso} 1.9715 is attributed to the positively charged six-co-ordinate oxo-Cr^V monochelate [Cr(O)(*cis*-O,O-lac)(H₂O)₃]⁺ monochelate (**IX**, Figure 10) and that at g_{iso} 1.9743 to the [Cr(O)(O¹,O²-lactobionato)(H₂O)₃]⁺ complex (**X**). The positive charge of these species is consistent with their appearance at high [H⁺], and coordination to the oxidized ligand agrees

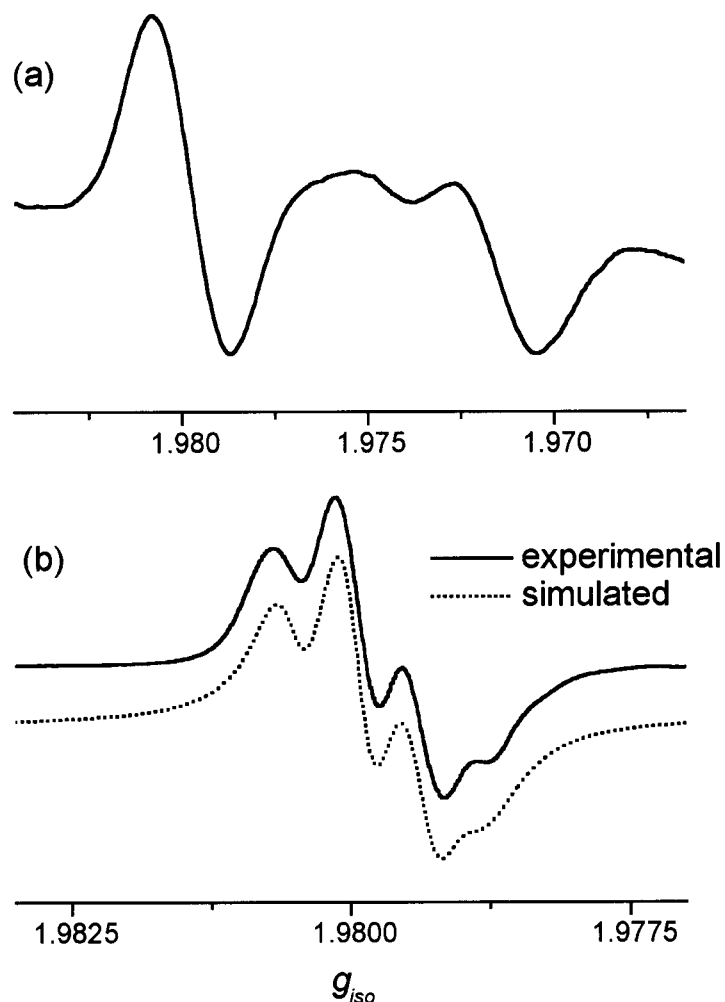


FIGURE 9. X-band EPR spectra of mixtures of (a) Cr^{VI}:lac = 1:33, [H⁺] = 0.20 M; $t = 6$ min, mod. ampl. = 4 G; (b) Cr^{VI}:lac = 1:19, pH = 5.0, $t = 24$ h, mod. ampl. = 0.4 G, $I = 1.0$ M, $T = 20$ °C, frequency ≈ 9.7 GHz.

with the fact that Cr^{VI} is a stronger oxidant in more acidic medium. Only the signal at g_{iso} 1.9797 persists at higher pH and could be deconvoluted into two triplets at g_{iso1} 1.9800 and g_{iso2} 1.9794 (A_{iso} $(16.5(3) \times 10^{-4} \text{ cm}^{-1})$, $\sim 50:50$ g_{iso1}/g_{iso2} ratio) (Figure 10-b). These EPR spectral parameters are consistent with those expected for any of the three linkage isomers of the $[\text{Cr}(\text{O})(\text{cis-}O, O\text{-lac})_2]^-$ (**XI** - **XIII**). In the reaction of Cr^{VI} with mal, the EPR spectra consist of two triplets at g_{iso} 1.9795 and 1.9794, which are attributed to the two geometric isomers of the $[\text{Cr}(\text{O})(O', O^2\text{-mal})_2]^-$ (**XII**), with mal bound to Cr^{VI} via the 1,2-*cis* diolate moiety. The EPR spectra of Cel/Cr^{VI} reaction mixtures consist of one triplet at g_{iso} 1.9793, which corresponds to the $[\text{Cr}(\text{O})(O', O^2\text{-Cel})_2]^-$ chelate (**XII**). In the reaction of Cr^{VI} with mel, the EPR spectra show two triplets at g_{iso1} 1.9802 and g_{iso2} 1.9798 ($\sim 50:50$ g_{iso1}/g_{iso2} ratio), corresponding to different linkage isomers of the five-coordinated oxo-Cr^V complex $[\text{Cr}(\text{O})(O, O\text{-mel})_2]^-$ (**XI** - **XIII**).

Species **XI** - **XIII** are also formed when Cr^V is generated by reaction of Cr^{VI} with GSH (1:1 ratio) at pH = 5.0 and stabilized by the presence of 10-times excess disaccharide over Cr^{VI} [56]. This result

evidences that Cr^{V} species observed at this pH effectively correspond to Cr^{V} chelates formed with the disaccharide and not with the oxidized product (aldobionic acid).

The fact that only Cr^{V} -disaccharide species are formed in the Cr^{VI} /disaccharide reaction at pH 3-7, indicates that the disaccharides are better chelating agents for Cr^{V} than aldoses. The latter are poorer complexation agents than the corresponding aldonic acids so that Cr^{V} -ald-ald and Cr^{V} ald₂ bis-chelates are the major species observed in the EPR spectra of the Cr^{VI} /aldose reaction mixtures.

2.8. Aldopentoses

The biological relevance of the interaction of Cr^{V} with diolate groups of furanoses was first pointed out in a work where it was shown that Cr^{V} complexation occurred with single ribonucleotide units but not with the analogous deoxyribonucleotides [57]. This suggested that the *cis*-diolate group of the ribose unit was involved in the Cr^{V} coordination. Cr^{V} species formed with ribonucleotides and with D-ribose 5'-monophosphate have been characterized and yield EPR spectroscopic parameters ($g_{\text{iso}} \approx 1.979$ and $A_{\text{iso}} \approx 16.3 \times 10^{-4} \text{ cm}^{-1}$) indicative of Cr^{V} -diolate binding [58]. The redox chemistry of the D-ribose (rib)/ Cr^{VI} system has been studied [59]. It was found that the reduction of Cr^{VI} by rib is six-times higher than that of allo -the aldohexose with the same configuration of C2 and C3-. The fact that the furanose ring favors oxidation vs complexation processes was interpreted as the consequence of the influence of the strain-induced instability of the chromate ester on the redox rate. This effect is enhanced in the reaction between Cr^{V} and the furanose, and can be evidenced when the observed rate constants for the reduction of Cr^{V} (k_5) and Cr^{VI} (k_6) by the aldose are compared for the pyranose and furanose forms. In the chromic oxidation of aldohexoses (pyranose form) in 0.75 M HClO_4 , k_5 are no more than 10-times higher than k_6 [49]; whereas for rib, $k_5 > 100 k_6$ [59]. The higher $k_{\text{ox}}/K_{\text{complexation}}$ ratio for the rib/ Cr^{VI} system, means that intramolecular electron transfer paths are faster within the less stable hypervalent chromium intermediate complexes.

The reaction of Cr^{VI} with an excess of rib, in the 4-6 pH range, yields an EPR spectrum dominated by a single detectable signal ($g_{\text{iso}} = 1.9787$, $A_{\text{iso}} 15.7 \times 10^{-4} \text{ cm}^{-1}$), corresponding to five-coordinated oxo- Cr^{V} complexes. In this pH range, Cr^{V} remains in solution several days. At low modulation amplitude, the shf pattern partially resolves, and the Cr^{V} EPR spectrum results to be a composite of several Cr^{V} species. Based on the EPR shf spectral pattern derived for the cyclopentane-1,2-diol/ Cr^{V} system the spectra can be deconvoluted into three signals with spectroscopic EPR parameters consistent with the presence of the $[\text{Cr}(\text{O})(\text{O}^{1(2)}, \text{O}^{2(3)}\text{-rib})(\text{O}^1, \text{O}^2\text{-riba})]^-$ ($g_{\text{iso}} 1.9791$ and 1.9792) and $[\text{Cr}(\text{O})(\text{O}^1, \text{O}^2\text{-riba})_2]$ ($g_{\text{iso}} 1.9785$) [59].

In $[\text{HClO}_4] \geq 0.1 \text{ M}$, the EPR spectra of the reaction of Cr^{VI} with excess rib show that six-coordinated oxo- Cr^{V} monochelates ($g_{\text{iso}} 1.9711$) form besides the five-coordinated oxo- Cr^{V} species at $g_{\text{iso}} 1.9787$ (Figure 11) [59], and they are the major Cr^{V} species in 0.15-1.0 M HClO_4 . Unlike that observed for pyranoses, the two Cr^{V} signals decay at different rates, and these rates increase with decreasing pH. Probably, the two types of complexes -five- and six-coordinated observed in the rib/ Cr^{VI} reaction are formed independently and yield the final Cr^{III} by two parallel paths.

2.9. 2-Deoxyaldoses

The study of the reaction of 2-deoxyaldoses with Cr^{VI} show that the lack of the C₂-OH group favors the redox reactions and reduce the capability of the aldose for binding hypervalent Cr [60,61].

The reaction of 2-deoxy-D-glucose (2dglc) and Cr^{VI} results in the formation of two Cr^{V} species with $g_{\text{iso}} 1.9781$ and 1.9754 in a 2.6 ratio independently of the pH and [2dglc] [61]. The two species disappear at comparable rates, meaning that these Cr^{V} intermediates are in rapid equilibrium compared to the time-scale of their subsequent reduction to Cr^{III} . The spectroscopic EPR parameters indi-

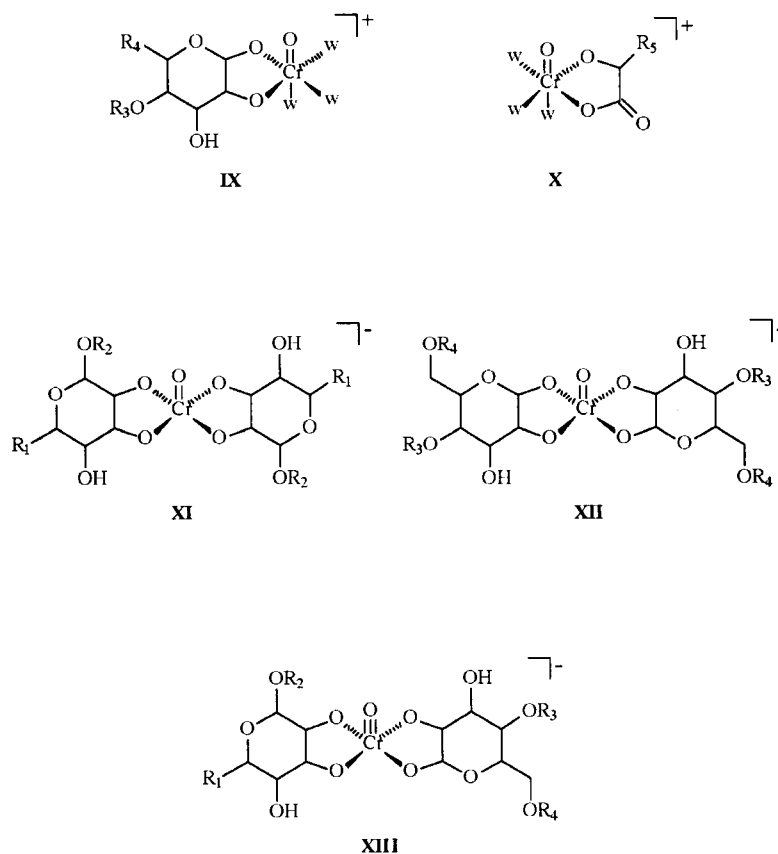


FIGURE 10. Oxo- Cr^{VI} mono- and bis-chelates formed in the reaction between Cr^{VI} and disaccharides. $R_1 = \text{CH}_2\text{OH}$. $\text{Cr}^{\text{VI}}\text{-Lac}_2$: $R_2 = \text{O}^4\text{-glc}$; $\text{Cr}^{\text{VI}}\text{-Mel}_2$: $R_2 = \text{O}^6\text{-glc}$. $\text{Cr}^{\text{VI}}\text{-Lac}_2$ ($\text{Cr}^{\text{VI}}\text{-Mal}_2$, $\text{Cr}^{\text{VI}}\text{-Cel}_2$): $R_3 = \text{glycoside}$, $R_4 = \text{H}$; $\text{Cr}^{\text{VI}}\text{-Mel}_2$: $R_3 = \text{H}$, $R_4 = \text{glycoside}$. $w = \text{water}$. $R_5 = \text{C}_{10}\text{O}_9\text{H}_{19}$.

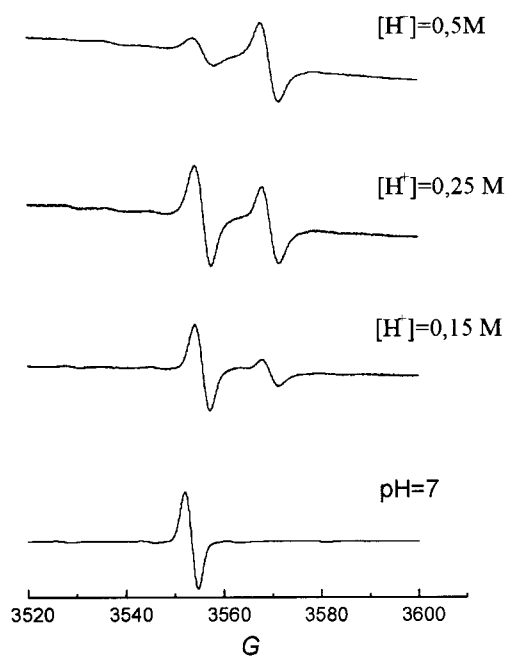


FIGURE 11. X-band EPR spectra of a mixture of rib and Cr^{VI} (10:1 mole ratio) at different $[\text{H}^+]$. $T = 20^\circ\text{C}$, mod. ampl. = 4 G, frequency $\approx 9.85\text{ GHz}$.

cate the signals can be assigned to Cr^{V} bis- and mono-chelates formed with the substrate: $[\text{Cr}(\text{O})(\text{O}^3, \text{O}^4\text{-2dglc})(\text{O}^1\text{-2dglc})(\text{H}_2\text{O})]^-$ ($g_{\text{calc}} 1.9783$) and $[\text{Cr}(\text{O})(\text{O}^1\text{-2dglc})(\text{H}_2\text{O})_3]^-$ ($g_{\text{calc}} 1.9756$).

2-acetamido-2-deoxy-D-glucose is oxidized by Cr^{VI} to the aldonic acid and the reaction is proposed to occur by a reaction path involving Cr^{V} . However, Cr^{V} intermediates could not be detected by EPR in the 0.15 – 1.0 M $[\text{H}^+]$ used in the kinetic measurements [62].

The reaction of Cr^{VI} with an excess of 2-deoxy-D-ribose (2drib), in the 4-7 pH range, yields only one Cr^{V} intermediate species, probably $[\text{Cr}(\text{O})(2\text{drib})(2\text{driba})]$, with $g_{\text{iso}} 1.9791$ and $A_{\text{iso}} 16.6 \times 10^{-4} \text{ cm}^{-1}$.⁵⁹ At pH 2, a minor signal with $g_{\text{iso}} 1.9735$ appears, and when the $[\text{H}^+] > 0.1 \text{ M}$ a third signal at $g_{\text{iso}} 1.9707$ is observed (Figure 12) [59]. The g_{iso} values of the two signals at higher field correspond to six-coordinated oxo- Cr^{V} complexes. The relative proportions of the three species depend essentially on the acidity. The two (or three) signals decay at comparable rates, and these rates increase with decreasing pH, such as observed for 2dglc.

2.10. Uronic acids

The redox reaction between Cr^{VI} and galacturonic acid has been studied and relatively long-lived Cr^{V} intermediates were found by EPR spectroscopy [26,43]. Galacturonic acid is oxidized by Cr^{VI} to mucic acid, when an excess of substrate over Cr^{VI} is used. The reaction is catalyzed by acid and proceeds through a $\text{Cr}^{\text{VI}} \rightarrow \text{Cr}^{\text{V}} \rightarrow \text{Cr}^{\text{III}}$ path [43]. When a large excess of galacturonic acid over Cr^{VI} is used (2000-7000 : 1), in the 1-6 pH range, the EPR signal is a composite of at least three five-coordinated oxo- Cr^{V} species, with $g_{\text{iso}} 1.9786$, 1.9785 and 1.9784 and $A_{\text{iso}} \approx 17.2 \times 10^{-4} \text{ cm}^{-1}$ (Figure 13). The EPR spectral parameters are indicative of the presence of three different isomers of $[\text{Cr}(\text{O})(\text{O}^5, \text{O}^6\text{-galacturonate})_2]$, with Cr^{V} bound to the carboxylato and alcoholate donor groups of the ligand [43].

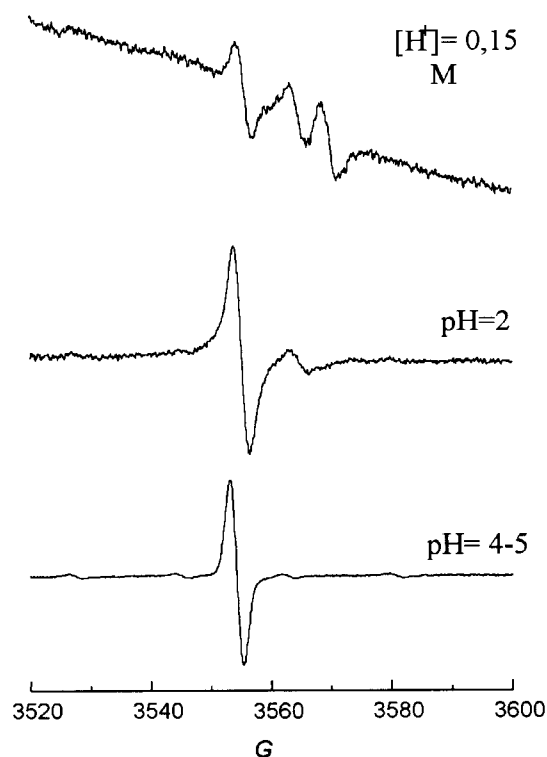


FIGURE 12. X-band EPR spectra of a mixture of 2drib and Cr^{VI} (10:1 mole ratio) at different $[\text{H}^+]$. $T = 20^\circ\text{C}$, mod. ampl. = 8 G, frequency $\approx 9.84 \text{ GHz}$.

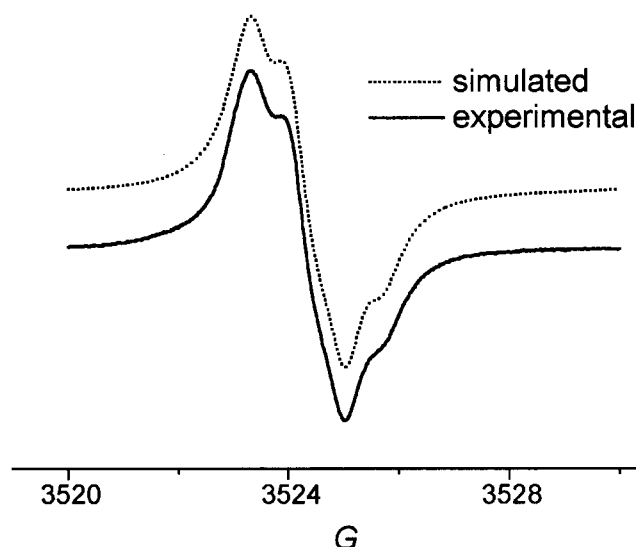


FIGURE 13. X-band EPR spectra of a mixture of Cr^V:galacturonic acid = 1:7000, pH 1.0, mod. ampl. = 0.3 G, $I = 1.0$ M, $T = 20$ °C, frequency = 9.7746 GHz.

3. Conclusions

The above results show that saccharides are effective complexation agents for Cr^V, affording very stable Cr^V-bis-chelates over a large range of pH values. Strong acid conditions ($[H^+] > 0.1$ M) are required to favor the redox reaction between the saccharide and Cr^V over the complexation by a second molecule of the substrate. The EPR spectroscopic studies of Cr^V-cyclic saccharides systems show that, when *cis*- and *trans*-diol groups are present in the saccharide, Cr^V prefers to bind the *cis*-diolato moieties, with very small to negligible proportion of species with Cr^V bound to the *trans*-diol groups. The 2-hydroxyacid donor groups are favored with respect to 1,2-diols for stabilizing Cr^V at low pH values (≈ 4), but the opposite is the case at pH ≈ 7 . At neutral pH, the Cr^V-2-hydroxycarboxylato complexes rapidly decompose by disproportionation, while Cr^V species formed *via* the *vic*-diolate moiety of saccharides are very stable and stay in solution for long time. Both the 2-hydroxycarboxylato and the *vic*-diolate moieties of saccharides compete effectively for complexation of Cr^V compared to GSH or cys at all the pH values studied.

ACKNOWLEDGEMENTS

We wish to thank all the collaborators who participated in the research and the National Research Council of Argentina (CONICET), the Third World Academy of Sciences (TWAS), the National University of Rosario (UNR), the International Foundation for Sciences (IFS) and Antorchas Foundation for the financial support.

REFERENCES

1. Klein, C. B. in *Toxicology of Metals*, Chang, L. W., ed., CRC-Lewis Publishers, New York, 1996, pp. 205-220.

2. Codd, R.; Dillon, C. T.; Levina, A.; Lay, P. A. *Coord. Chem. Rev.* **2001**, 216-217, 533-577.
3. Katz, S. A.; Salem, H. *The Biological and Environmental Chemistry of Chromium*, VCH Publishers. Inc., New York, 1994, pp. 65-119.
4. Shi, X.; Chiu, A.; Chen, C. T.; Halliwell, B.; Castranova, V.; Vallyathan, V. J. *Toxicol. Environm. Health, Part B*, **1999**, 87-104.
5. Costa, M. *Crit. Rev. Toxicol.* **1997**, 27, 431-442.
6. Gould, E. S. *Coord. Chem. Rev.* **1994**, 135/136, 651-684.
7. Zhang, L.; Lay, P. A. *J. Am. Chem. Soc.* **1996**, 118, 12624-12637.
8. Geiger, D. K. *Coord. Chem. Rev.* **1997**, 164, 261-288.
9. Levina, A.; Lay, P. A.; Dixon, N. E. *Inorg. Chem.* **2000**, 39, 385-395.
10. Stearns, D. H.; Wetterhahn, K. E. *Chem. Res. Toxicol.* **1994**, 7, 219-230.
11. Wetterhahn Jannette, K. E. *J. Am. Chem. Soc.* **1982**, 104, 874-875.
12. O'Brien, P.; Barrett, J.; Swanson, F. *Inorg. Chim. Acta* **1985**, 108, L19-L20.
13. Lay, P. A.; Levina, A. *J. Am. Chem. Soc.* **1998**, 120, 6704-6714.
14. Ciésłak-Golonka, M. *Polyhedron* **1996**, 15, 3667-3689.
15. Zhang, L.; Lay, P. A. *Aust. J. Chem.* **2000**, 53, 7-13.
16. S. Signorella, C. Palopoli, M. Santoro, S. García, V. Daier, J. C. González, V. Roldán, M. I. Frascaroli, M. Rizzotto, L. F. Sala; *Research Trends*, in press
17. Mehta, N.; Dubach, P.; Deuel, H. *Adv. Carbohydr. Chem. Biochem.*, Vol. 16, **1958**, 335-355.
18. Barr-David, G.; Charara, M.; Codd, R.; Farrell, R. P.; Irwin, J. A.; Lay, P. A.; Bramley, R.; Brumby, S.; Ji, J.-Y.; Hanson, G. R. *J. Chem. Soc., Faraday Trans.* **1995**, 91, 1207-1216.
19. Bramley, R.; Ji, J.-Y.; Judd, R. J.; Lay, P. A. *Inorg. Chem.* **1990**, 29, 3089-3094.
20. Farrell, R. P.; Judd, R. J.; Lay, P. A.; Bramley, R.; Ji, J.-Y. *Inorg. Chem.* **1989**, 28, 3401-3403.
21. Codd, R.; Lay, P. A. *J. Am. Chem. Soc.* **1999**, 121, 7864-7876
22. Signorella, S.; Daier, V.; Santoro, M.; García, S.; Palopoli, C.; González, J. C.; Korecz, L.; Rockenbauer, A.; Sala, L. F. *Eur. J. Inorg. Chem.* **2001**, 1829-1833.
23. Israeli, Y.; Detellier, C. *Carbohydr. Res.* **1997**, 297, 201-207
24. Mitewa, M.; Bontchev, P. *Coord. Chem. Rev.*, **1985**, 61, 241-272.
25. Kaiwar, S. P.; Raghavan, M. S. S.; Rao, C. P. *Carbohydr. Res.*, **1994**, 256, 29-40.
26. Branca, M.; Micera, G.; Dessi, A. *Inorg. Chim. Acta*, **1988**, 153, 61-65.
27. Roldán, V.; Daier, V.; Goodman, B.; Santoro, M.; González, J. C.; Calisto, N.; Signorella, S.; Sala, L. *Helv. Chim. Acta*, **2000**, 83, 3211-3228.
28. Bramley, R.; Ji, J.-Y.; Lay, P. A. *Inorg. Chem.* **1991**, 30, 1557-1564.
29. Branca, M.; Micera, G.; Segre, U.; Dessi, A. *Inorg. Chem.* **1992**, 31, 2404-2408.
30. González, J. C.; Signorella, S.; Sala, L. F., unpublished results.
31. Signorella, S.; Frascaroli, M. I.; García, S.; Santoro, M.; González, J. C.; Palopoli, C.; Casado, N.; Sala, L. F. *J. Chem. Soc., Dalton Trans.* **2000**, 1617-1623.
32. Rizzotto, M.; Levina, A.; Santoro, M.; García, S.; Frascaroli, M. I.; Signorella, S.; Sala, L. F.; Lay, P. A., unpublished results.
33. Lay, P. A.; Levina, A. *Inorg. Chem.* **1996**, 35, 7709-7717.
34. Sugden, K. D.; Wetterhahn, K. E. *Chem. Res. Toxicol.* **1997**, 10, 1397-1405.
35. Levina, A.; Barr-David, G.; Codd, R.; Lay, P. A.; Dixon, N. E.; Hammershøi, A.; Hendry, P. *Chem. Res. Toxicol.* **1999**, 12, 371-381.
36. Krumpolc, M.; DeBoer, B. G.; RoĚek, J. *J. Am. Chem. Soc.* **1978**, 100, 145-153.
37. Krumpolc, M.; RoĚek, J. *J. Am. Chem. Soc.* **1979**, 101, 3206-3209.
38. Judd, R. J.; Hambley, T. W.; Lay, P. A. *J. Chem. Soc., Dalton Trans.* **1989**, 2205-2210.
39. Branca, M.; Dessi, A.; Micera, G.; Sanna, D. *Inorg. Chem.* **1993**, 32, 578-581.
40. Signorella, S.; García, S.; Sala, L. F. *Polyhedron* **1992**, 11, 1391-1396.
41. Codd, R.; Levina, A.; Zhang, L.; Hambley, T. W.; Lay, P. A. *Inorg. Chem.* **2000**, 39, 990-997.
42. Haight, G.; Jwisich, G.; Kelso, M.; Merril, P. *Inorg. Chem.*, **1985**, 24, 2740-2746.
43. González, J. C.; Signorella, S.; Goodman, B.; Daier, V., unpublished results.
44. Signorella, S.; Santoro, M.; Palopoli, C.; Brondino, C.; Salas-Peregrin, J. M.; Quirós M.; Sala, L. F. *Polyhedron*, **1998**, 17, 2739-2749.
45. Signorella, S.; Santoro, M. I.; Mulero, M.; Sala, L. F. *Can. J. Chem.* **1994**, 72, 398-402.
46. Signorella, S.; García, S.; Sala, L. F. *Polyhedron* **1997**, 16, 701-706.
47. Palopoli, C.; Signorella, S.; Sala, L. F. *New J. Chem.* **1997**, 21, 343-348.
48. Signorella, S.; Lafarga, R.; Daier, V.; Sala, L. F. *Carbohydr. Res.* **2000**, 324, 127-135.

49. Signorella, S.; Daier, V.; García, S.; Cargnello, R.; González, J. C.; Rizzotto, M.; Sala, L. F. *Carbohydr. Res.* **1999**, *316*, 14-25.
50. Signorella, S.; García, S.; Sala, L. F. *J. Chem. Ed.* **1999**, *76*, 405-408.
51. Sala, L. F.; Signorella, S.; Rizzotto, M.; Frascaroli, M. I.; Gandolfo, F. *Can. J. Chem.* **1992**, *70*, 2046-2052.
52. Branca, M.; Dessi, A.; Kozłowski, H.; Micera, G.; Swiatek, J. *J. Inorg. Biochem.* **1990**, *39*, 217-226.
53. Rizzotto, M.; Frascaroli, M. I.; Signorella, S.; Sala, L. F. *Polyhedron* **1996**, *15*, 1517-1523.
54. Lay, P. A., personal communication.
55. Goodgame, D. M. L.; Joy, A. M. *Inorg. Chim. Acta* **1987**, *135*, L5-L7.
56. Roldán, V.; González, J. C.; Santoro, M.; García, S.; Casado, N.; Olivera, S.; Salas-Peregrin, J. M.; Signorella, S.; Sala, L. F., unpublished results.
57. Goodgame, D. M. L.; Hayman, P. B.; Hathway, D. E. *Polyhedron* **1982**, *1*, 497-499.
58. Rizzotto, M.; Moreno, V.; Signorella, S.; Daier, V.; Sala, L. F. *Polyhedron* **2000**, *19*, 417-423.
59. Daier, V.; Signorella, S.; Rizzotto, M.; Frascaroli, M. I.; Palopoli, C.; Brondino, C.; Salas-Peregrin, J. M.; Sala, L. F. *Can. J. Chem.* **1999**, *77*, 57-64.
60. Rizzotto, M.; Signorella, S.; Frascaroli, M. I.; Daier, V.; Sala, L. F. *J. Carbohydr. Chem.* **1995**, *14*, 45-51.
61. Signorella, S.; Rizzotto, M.; Daier, V.; Frascaroli, M. I.; Palopoli, C.; Martino, D.; Bousseksou, A.; Sala, L. F. *J. Chem. Soc., Dalton Trans.* **1996**, 1607-1611.
62. Sala, L. F.; Palopoli, C.; Signorella, S. *Polyhedron* **1995**, *14*, 1725-1730.